PALEOCEANOGRAPHY, VOL. 23, PA3101, doi:10.1029/2008PA001620, 2008

El Niño–Southern Oscillation–like variability during glacial terminations and interlatitudinal teleconnections

L. D. Pena,[1] I. Cacho,[1] P. Ferretti,[2] and M. A. Hall[2]

Received 5 March 2008; accepted 27 May 2008; published 29 July 2008.

[1] Interannual-decadal variability in the equatorial Pacific El Niño–Southern Oscillation (ENSO) induces climate changes at global scale, but its potential influence during past global climate change is not yet well constrained. New high-resolution eastern equatorial Pacific proxy records of thermocline conditions present new evidence of strong orbital control in ENSO-like variability over the last 275,000 years. Recurrent intervals of saltier thermocline waters are associated with the dominance of La Niña–like conditions during glacial terminations, coinciding with periods of low precession and high obliquity. The parallel dominance of δ^{13}C-depleted waters supports the advection of Antarctic origin waters toward the tropical thermocline. This "oceanic tunneling" is proposed to have reinforced orbitally induced changes in ENSO-like variability, composing a complex high- and low-latitude feedback during glacial terminations.

Citation: Pena, L. D., I. Cacho, P. Ferretti, and M. A. Hall (2008), El Niño–Southern Oscillation–like variability during glacial terminations and interlatitudinal teleconnections, *Paleoceanography*, *23*, PA3101, doi:10.1029/2008PA001620.

1. Introduction

[2] High-latitude regions have traditionally attracted most of the research attention addressing feedback processes involved in glacial-interglacial changes [*Cane*, 1998] whereas tropical regions have often been regarded as passive players in the course of past global climatic variability. Nowadays, we have unambiguous evidences demonstrating that the quasi regular phenomenon of El Niño–Southern Oscillation (ENSO), which operates at interannual-to-decadal timescales, is able to amend regional winds and precipitation patterns globally [*Fedorov and Philander*, 2000; *Wang and Fiedler*, 2006]. However, little is known about the role of the ENSO-like variability at glacial-interglacial timescales. Modeling studies suggest that ENSO-like variability is sensitive to orbital forcing, in particular to the effect that the orbital precession exerts on the tropics [*Clement et al.*, 1999, 2000]. At present, the number of tropical records which can evaluate the mean state of ENSO on orbital timescales is still limited [*Beaufort et al.*, 2001; *Ravelo et al.*, 2006]. Most interest has been dedicated to suborbital timescales [*Clement et al.*, 2000; *Koutavas et al.*, 2006; *Stott et al.*, 2002], particularly to the study of the ENSO-like variability over the last deglaciation. Evidences so far are conflicting; some studies consider the period of global deglaciation an "El Niño-like" state of climate whereas others infer "La Niña-like" conditions for the same period [*Andreasen et al.*, 2001; *Beaufort et al.*, 2001; *Koutavas et al.*, 2006, 2002; *Stott et al.*, 2002]. This study provides high-resolution paleoceanographic records from the eastern equatorial Pacific (EEP) that supports ENSO-like variability from multicentennial to orbital scales and enable a new assessment of the tropical Pacific role in past global climate changes.

[1]GRC Geociències Marines, Department of Stratigraphy, Paleontology and Marine Geosciences, University of Barcelona, Barcelona, Spain.

[2]Godwin Laboratory for Palaeoclimate Research, Department of Earth Sciences, University of Cambridge, Cambridge, UK.

0883-8305/08/2008PA001620$12.00

2. Methods

[3] Multiproxy records were established at Site 1240 (Ocean Drilling Program (ODP) Leg 202) from the northern flank of Carnegie Ridge (0°01.31′N, 86°27.76′W; 2,921 m water depth) in the Panama Basin (Figure 1a). One of the main oceanographic features at this location is the Equatorial Undercurrent (EUC), an eastward flowing subsurface current (50–300 m water depth) that transports thermocline waters from the western Pacific along the equator [*Lukas*, 1986; *Tsuchiya et al.*, 1989] (Figures 1b–1d). Paired stable isotope (δ^{18}O, δ^{13}C) and trace element (Mg/Ca) measurements [*Pena et al.*, 2005] were carried out on two planktonic foraminifera species (*Globigerinoides ruber* and *Neogloboquadrina dutertrei*) that inhabit surface and thermocline depths, respectively [*Fairbanks et al.*, 1982]. The records therefore enable reconstruction of past EEP surface and thermocline properties. The age scale for Site 1240 was constructed from 17 accelerator mass spectrometry (AMS) ^{14}C ages and graphical tuning of the deeper parts of the records to Vostok ice core paleoclimatic profile (auxiliary material Table S1).[1] Unprecedented high sedimentation rates at the site of 6.4–25.2 cm ka^{-1} allow to establish fine-scale records (80–312 years per sample) that cover the last 275,000 years (275 ka) (see auxiliary material).

3. Results and Discussion

[4] Glacial-interglacial amplitudes along the *G. ruber* δ^{18}O record range from 1.3 to 2.7‰ (Figure 2b), whereas

[1]Auxiliary materials are available in the HTML. doi:10.1029/2008PA001620.

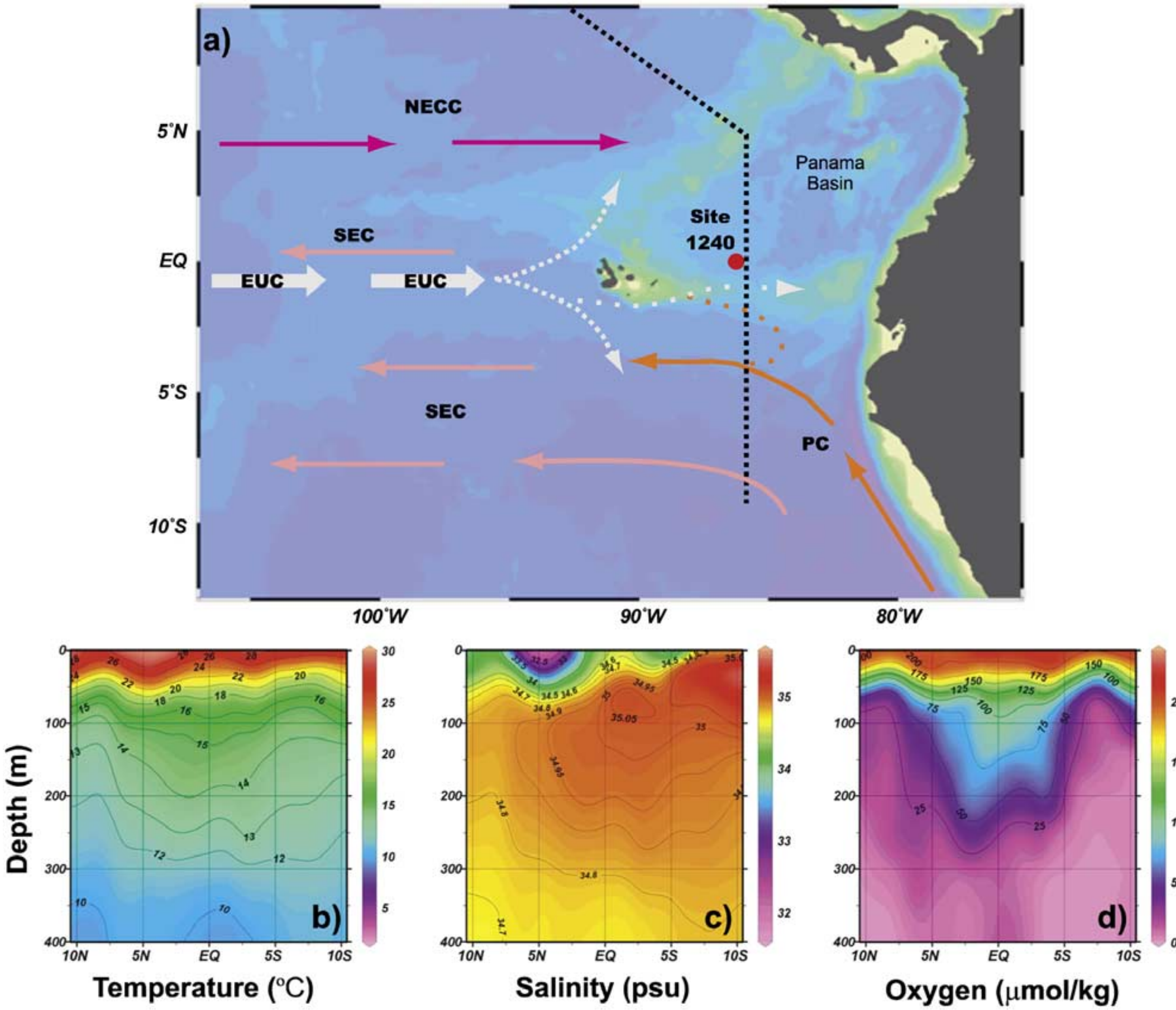

Figure 1. (a) Location of Ocean Drilling Program (ODP) 1240 (0°01.31′N, 86°27.76′W, and 2921 m water depth) in the Panama Basin. Schematic view of annual mean currents systems in the EEP: NECC, North Equatorial Counter Current; SEC, South Equatorial Current; EUC, Equatorial Undercurrent; and PC, Perú Current. World Ocean Circulation Experiment (WOCE) P19 transect is indicated by dashed line. (b–d) WOCE P19 during March 1993. The upper (400 m) thermal, salinity, and oxygen structure of this hydrographic section are shown [*Conkright et al.*, 2002].

the Mg/Ca–derived sea surface temperatures (SSTs) range from 3.2 to 4.5°C (Figure 2c) confirming similar variations previously reported in the area [*Lea et al.*, 2000]. SSTs lead δ^{18}O changes by 1 to 3 ka during glacial terminations, also in agreement with records from the EEP [*Lea et al.*, 2000] and the Southern Ocean [*Mashiotta et al.*, 1999]. Moreover, core top SST estimates derived from *G. ruber* of 24.8 ± 1.2°C agree with the mean SST of the nonupwelling season (25.1°C) [*Conkright et al.*, 2002] when *G. ruber* is known to calcify [*Fairbanks et al.*, 1982; *Thunell and Reynolds*, 1984]. The *N. dutertrei* δ^{18}O record exhibits reduced glacial-interglacial amplitudes (0.8–1.4‰) (Figure 2d), and the corresponding deep thermocline temperature (DTT) shows moderate warming (1.9–3.4°C) during terminations (Figure 2e). The core top temperature estimate for the DTT is 13.7±1.3°C which is typically encountered at 150–200 m in the water column [*Conkright et al.*, 2002] (auxiliary material Figure S1). This depth range is immediately below the modern EEP thermocline and corresponds to the main core of the EUC (Figures 1b–1d) [*Lukas*, 1986]. In order to acquire more information about the paleoceanographic evolution at Site 1240 we have calculated the deep thermocline seawater δ^{18}O estimate (DT-$\delta^{18}O_{sw}$), as a proxy of local salinity changes (Figure 2f). The DT-$\delta^{18}O_{sw}$ calculation involved the subtraction of the temperature effect (DTT) from the *N. dutertrei* δ^{18}O record and the removal of the global sea level component [*Waelbroeck et al.*, 2002] of the seawater δ^{18}O composition. A relative change of 1 ± 0.4‰ in the DT-$\delta^{18}O_{sw}$ composition corresponds to a salinity change of ~2.1 ± 0.7 practical salinity units (psu)

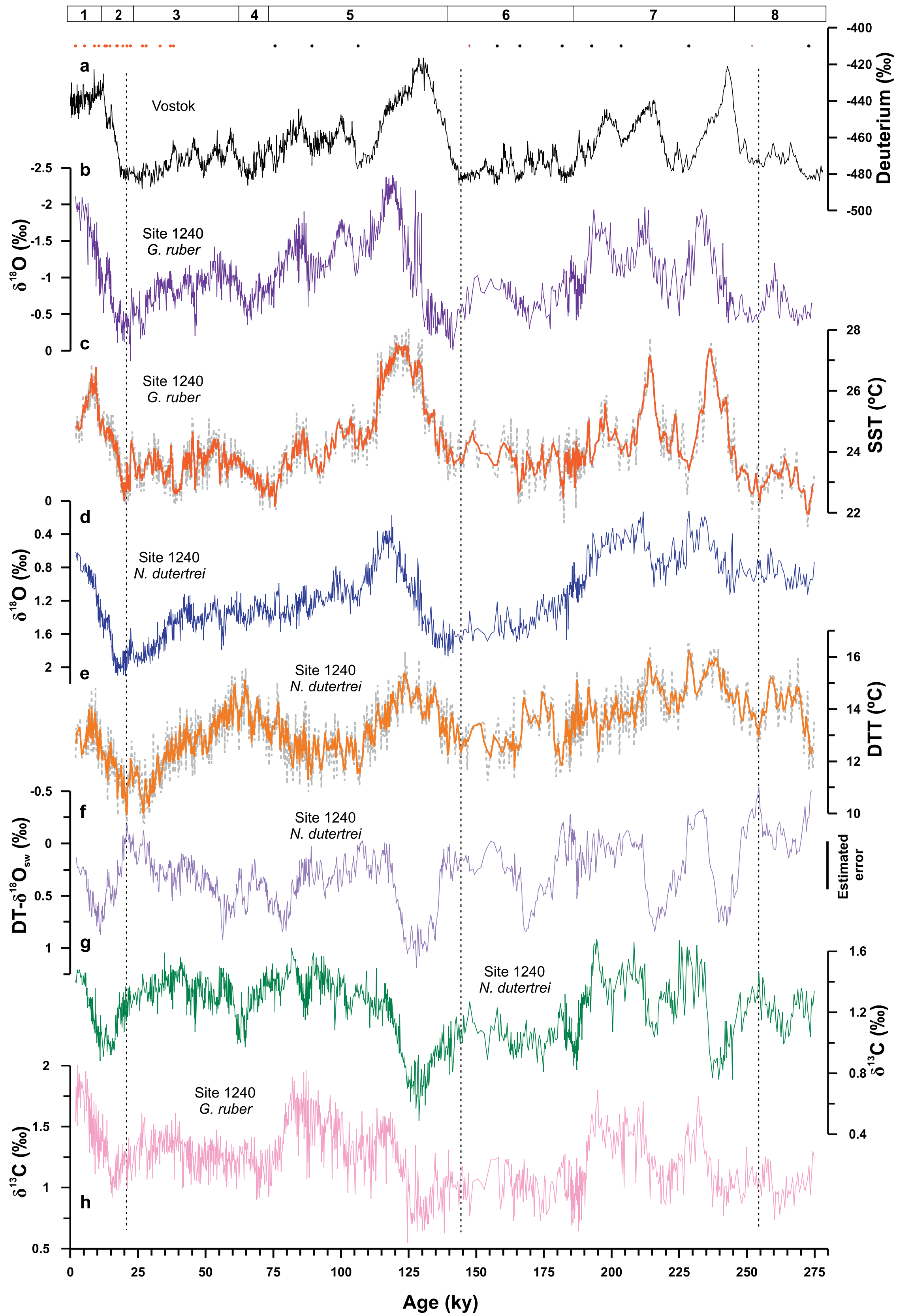
1
2
3
4
5
6
7
8
a
Vostok
Deuterium (‰)
b
Site 1240
G. ruber
δ18O (‰)
c
Site 1240
G. ruber
SST (ºC)
d
Site 1240
N. dutertrei
δ18O (‰)
e
Site 1240
N. dutertrei
DTT (ºC)
f
Site 1240
N. dutertrei
DT-δ18Osw (‰)
Estimated error
g
Site 1240
N. dutertrei
δ13C (‰)
h
Site 1240
G. ruber
δ13C (‰)
Age (ky)

Figure 2

[*Rohling*, 2007] (auxiliary material). Thus, more positive values of DT-$\delta^{18}O_{sw}$ indicate saltier waters at the thermocline whereas more negative DT-$\delta^{18}O_{sw}$ implies fresher waters. The obtained DT-$\delta^{18}O_{sw}$ record shows a set of positive events (up to 1.4‰) occurring during periods of relative warming at the thermocline, being particularly significant during terminations (Figure 2f). The advent of saltier and relatively warm waters in the thermocline is consistent with a strengthening of the EUC, which promotes a thickening of the thermostad and the arrival of high-salinity waters in the core of the EUC that is usually accompanied by downwelling of the upper layer thermal structure [*Lukas*, 1986]. These DT-$\delta^{18}O_{sw}$ positive events correlate significantly with substantial negative excursions in the *N. dutertrei* and *G. ruber* $\delta^{13}C$ records during terminations (Figures 2g and 2h), indicating upwelling from the thermocline to the surface.

[5] The down-core DT-$\delta^{18}O_{sw}$ record displays maxima/minima (enhanced/reduced upwelling) that correlate with precession minima/maxima (perihelion during Northern Hemisphere summer/winter) at a reasonably constant phase-lag relationship (DT-$\delta^{18}O_{sw}$ lags precession by 2.2 ka, as computed from cross-correlation analysis) (Figures 3a–3b and auxiliary material Figures S3c and S3d). That means that the insolation (and seasonal cycle) is the primary forcing with the modulation provided by the precession of the equinoxes. Model simulations indicate that increased insolation (perihelion) driven by precession reinforces the seasonally asymmetric wind field above the equator [*Clement et al.*, 1999]. During summer, the Intertropical Convergence Zone (ITCZ) moves northward over the EEP and the wind field becomes divergent in the east while remaining convergent in the west. This situation promotes a strong E-W asymmetry in oceanic and atmospheric heating that drives easterly wind anomalies (enhanced Walker circulation) and establishes La Niña–like conditions in the EEP [*Clement et al.*, 1999]. Accordingly, we interpret positive DT-$\delta^{18}O_{sw}$ intervals as La Niña–like conditions in the sense of reflecting mean states in which La Niña conditions are more frequent and/or more intense.

[6] Precession is the prevailing signal in the DT-$\delta^{18}O_{sw}$ record but there is also strong and significant spectral power around the obliquity band (Figures 3c–3d and auxiliary material Figure S3a and S3b). Periods of high obliquity coincide with more positive DT-$\delta^{18}O_{sw}$ values but with a rather variable phase relationship and different amplitude modulation. This unexpectedly strong obliquity signal has also been observed in a number of tropical Pacific records [*Lea et al.*, 2000]. Given that the low-latitude insolation forcing due to obliquity is relatively small (<3 W m^{-2}), the 41 ka periodicities in tropical marine proxy records are unlikely to arise as a direct climate response to the obliquity component of local insolation [*Lee and Poulsen*, 2005]. Indeed, some periods that would be expected to show large positive DT-$\delta^{18}O_{sw}$ events at 110, 150 and 190 ka, in view of low-precession values, are actually recording minor or absent DT-$\delta^{18}O_{sw}$ events coinciding with relatively low-obliquity values (Figure 3). Thus, according to these results, precession can be seen as the pacemaker of the EEP DT-$\delta^{18}O_{sw}$ variations with obliquity acting to modulate the signal amplitude. Such relationship is clearly illustrated during terminations (Figures 3e–3g), when the existing orbital configurations (low precession and high obliquity) promoted the largest DT-$\delta^{18}O_{sw}$ excursions corresponding to sustained and/or strong upwelling (La Niña–like) periods in the EEP. It has been suggested that this obliquity imprint may have propagated from high-to-low latitudes via atmospheric teleconnections [*Chiang and Lintner*, 2005] or through thermocline circulation via the so-called "oceanic tunnel" [*Bostock et al.*, 2004; *Fedorov et al.*, 2006; *Lee and Poulsen*, 2005]. Further support to the idea that obliquity forcing propagated through tropical thermocline rather than through atmospheric changes, emerges from the occurrence of intense negative $\delta^{13}C$ excursions at the EEP thermocline preceding the last three terminations (Figure 2g). This persistent feature of planktonic foraminiferal records from Indo-Pacific, south Atlantic and sub-Antarctic records [*Ninnemann and Charles*, 1997; *Shackleton et al.*, 1983; *Spero and Lea*, 2002] suggests a southern source for this signal. At Site 1240, $\delta^{13}C$ minima are similar in amplitude and duration to previously published $\delta^{13}C$ records from nearby cores [*Shackleton et al.*, 1983; *Spero and Lea*, 2002]. Interestingly, the onset of the *N. dutertrei* $\delta^{13}C$ negative excursions is synchronous in time with the DTT warming (see auxiliary material Figure S4). *Spero and Lea* [2002] suggest that $\delta^{13}C$ minima in glacial terminations in the EEP derive from Southern Ocean deep water mass as transmitted into the Indo-Pacific thermocline via the Sub-Antarctic Mode Water/Antarctic Intermediate Water (SAMW/AAIW). Although the oceanic pathways between the Sub-Antarctic water masses and tropical thermocline are not well constrained, it is clear that the waters transported by the EUC are mostly fed by sub-Antarctic water masses [*Lukas*, 1986; *Tsuchiya et al.*, 1989], particularly by SAMW formed north of the sub-Antarctic front [*Toggweiler et al.*, 1991] (Figure 4). During glacial periods, the combination of weaker thermohaline circulation and increased circum-Antarctic ice-induced stratification resulted in a reduced

Figure 2. Records from ODP 1240 over the past 275 ka. (a) Antarctic Vostok deuterium (δD) (see auxiliary material). (b) *G. ruber* $\delta^{18}O$ record. (c) *G. ruber* $SST_{Mg/Ca}$. (d) *N. dutertrei* $\delta^{18}O$ record. (e) *N. dutertrei* $DTT_{Mg/Ca}$. (f) Calculated DT-$\delta^{18}O_{sw}$ (‰ Vienna SMOW), after removal of global ice volume effect, as a proxy for relative salinity changes in the EEP thermocline. Vertical bar indicates associated error ±0.45‰. (g and h) The $\delta^{13}C$ records measured on *N. dutertrei* and *G. ruber*, respectively. Oxygen and carbon isotopic values are in ‰ (Vienna Peedee belemnite). Age control points along the top axis are ^{14}C AMS (red), SST tie points to the Vostok deuterium record (black), and *N. dutertrei* $\delta^{13}C$ tie points to the Vostok CO_2 record for terminations II and III (purple) (see auxiliary material). Marine isotopic stages (MIS) 1–8 are labeled for reference. Vertical dashed lines indicate the onset of DTT warming associated to the last three terminations. A three-point moving average filter was applied to SST, DTT, and DT-$\delta^{18}O_{sw}$.

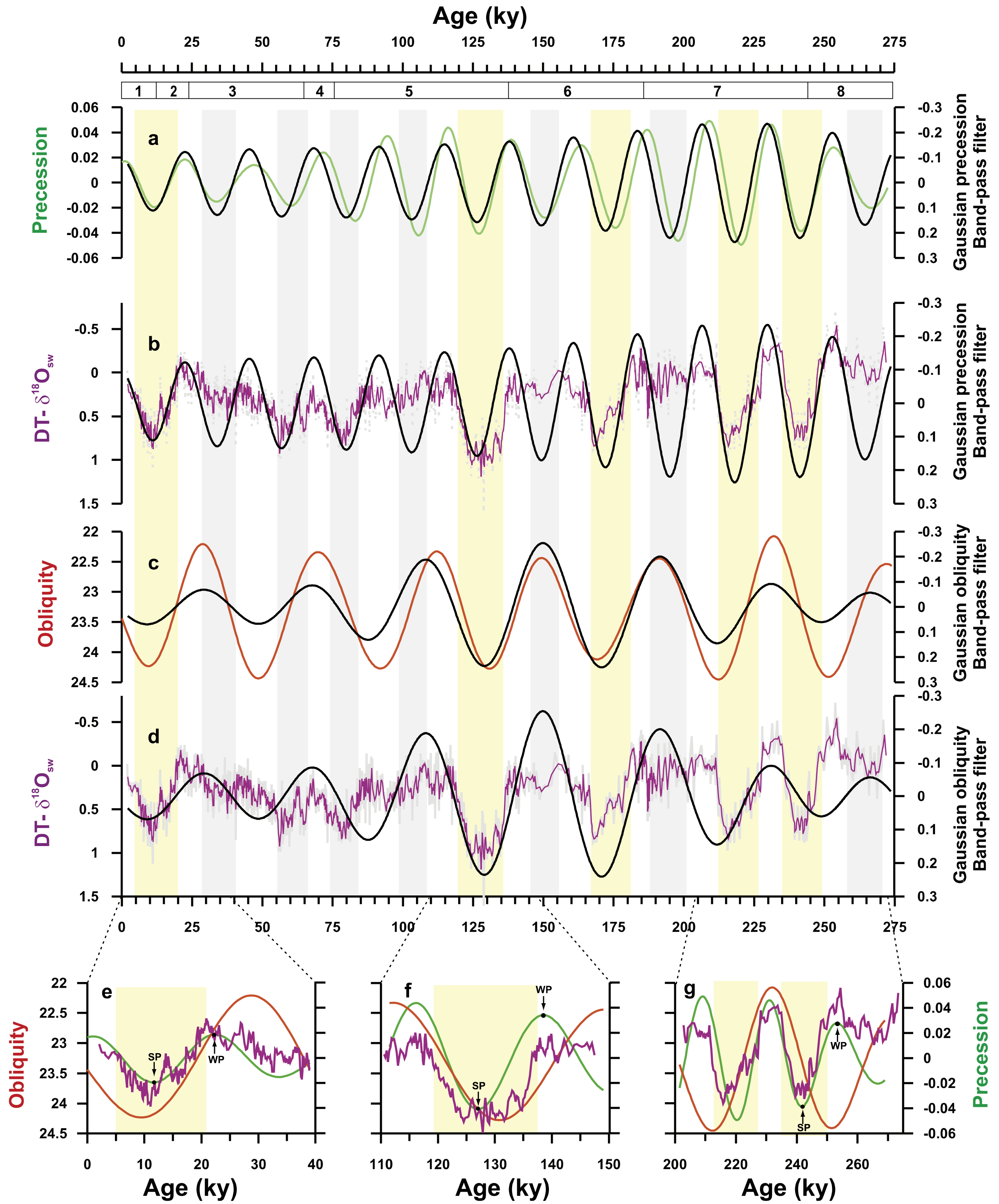
Age (ky)
a
b
c
d
e
f
g
Precession
DT- $\delta^{18}O_{sw}$
Obliquity
Gaussian precession Band-pass filter
Gaussian obliquity Band-pass filter
SP
WP
Age (ky)

Figure 3

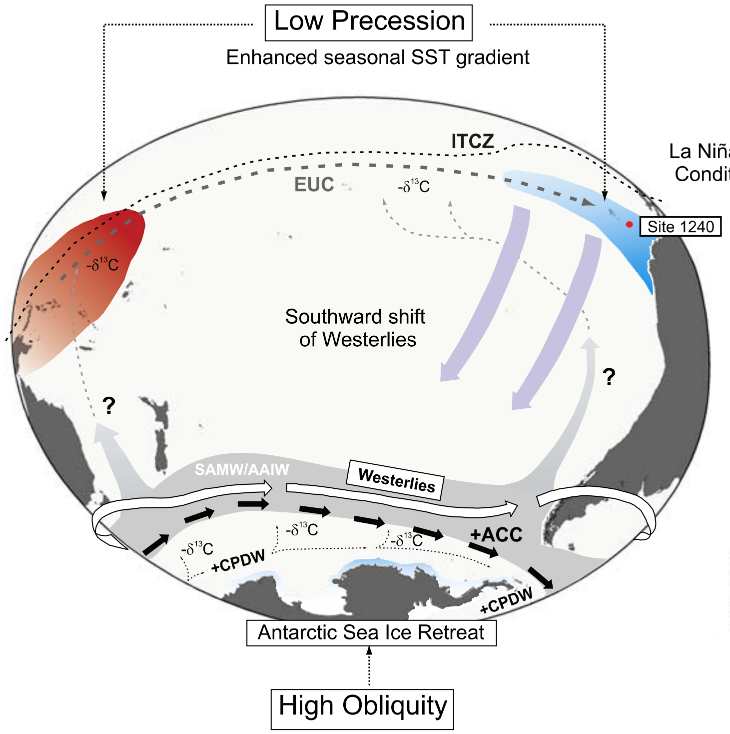

Figure 4. Schematic illustration of the discussed oceanic and atmospheric feedback processes that acted as a high- and low-latitude teleconnection mechanism during glacial terminations. The asymmetric seasonal insolation during low-precession periods enhances the tropical Pacific E-W SST gradient, eventually developing La Niña–like conditions in the EEP. These conditions promote a southward shift of the westerlies, which in combination with a reduced circum-Antarctic sea ice (high obliquity) produce an intensification of the Antarctic Circumpolar Current (ACC) and a resumption of the Circumpolar Deep Water (CPDW) upwelling. Finally, the Southern Ocean signal ($-\delta^{13}C$) is transmitted through intermediate waters mostly Sub-Antarctic Mode Water (SAMW) into tropical thermocline and incorporated in the EUC. However, the precise pathways for this "tunneling" of intermediate waters have not been well constrained yet. ITCZ is Intertropical Convergence Zone; AAIW is Antarctic Intermediate Water.

ventilation and $\delta^{13}C$ depletion of lower Circumpolar Deep Water (CPDW) [*Stephens and Keeling*, 2000; *Toggweiler*, 1999]. However, during terminations, Antarctic sea ice starts to withdraw because of increased seasonal insolation (high obliquity), at the time that the EEP shows predominant La Niña–like conditions (low precession) which promote a southward shift of the westerlies (Figure 4). This interpretation is supported by modeling studies [*Toggweiler*, 1999; *Toggweiler et al.*, 2006] and has been recently confirmed by a compilation of meteorological satellite information during El Niño and La Niña periods [*Yuan*, 2004] (see auxiliary material Figure S2). A southward displacement of the westerlies would reinforce the Antarctic Circumpolar Current (ACC) around Antarctica and, therefore, stimulate the resumption of the Southern Ocean upwelling system during terminations [*Toggweiler et al.*, 2006]. This would cause first upwelling [*Stephens and Keeling*, 2000] and eventually a northward advection of low $\delta^{13}C$ waters into the sub-Antarctic front where the SAMW/AAIW is formed [*Bostock et al.*, 2004]. The changes in the water column chemistry at the sub-Antarctic front are recorded in the chemistry of EEP foraminifera

Figure 3. Relationship between DT-$\delta^{18}O_{sw}$ record and the orbital parameters. (a) Comparison of precession versus DT-$\delta^{18}O_{sw}$ band-pass Gaussian filter in the precession band (0.0435 ka^{-1} and band width of 0.005 ka^{-1}). (b) DT-$\delta^{18}O_{sw}$ record versus DT-$\delta^{18}O_{sw}$ band-pass Gaussian filter in the precession band. (c) Comparison of obliquity versus DT-$\delta^{18}O_{sw}$ band-pass Gaussian filter in the obliquity band (0.0244 ka^{-1} and band width of 0.005 ka^{-1}). (d) DT-$\delta^{18}O_{sw}$ record versus DT-$\delta^{18}O_{sw}$ band-pass Gaussian filter in the obliquity band. (e–g) Detailed views of terminations I–III, respectively, in DT-$\delta^{18}O_{sw}$ compared to orbital precession and obliquity. SP and WP stand for summer and winter perihelion, respectively. Yellow bands correspond to major DT-$\delta^{18}O_{sw}$ excursions, whereas gray bands relate to minor events. The choice of band widths in the range of 0.003–0.01 ka^{-1} does not appreciably affect the Gaussian filters outputs.

within a century or less [*Tsuchiya*, 1991], thus establishing a nearly synchronous high- and low-latitude oceanographic link between the EEP and Antarctica (Figure 4).

4. Conclusions

[7] Our results from Site 1240 demonstrate that precession was the dominant forcing controlling past changes in the EEP upwelling intensity and that the obliquity signal at high latitudes acted as an amplifier-inhibitor mechanism of the low-latitude precession forcing. These high- and low-latitude teleconnections occur through the atmosphere by latitudinal shifts in winds belts and through the ocean by propagation of intermediate water masses from polar regions into tropical thermocline waters. This study provides new insights on the causes of glacial terminations and highlights the relevance of ENSO-like dynamics as an active positive feedback mechanism in both high- and low-latitude changes. This EEP–Southern Ocean linkage needs to be further implemented in climate models of past reconstructions and future predictions.

[8] **Acknowledgments.** Special thanks go to Nick J. Shackleton for supporting and stimulating this research. We acknowledge support from the Gary Comer Science and Education Foundation (COMER), NERC, UK-ODP, the "Ramón y Cajal" program (MEC-Spain), and GRC Geociències Marines is supported by the Generalitat de Catalunya program for excellence in research groups (ref. 2005SGR00152). This work was supported in part by the Spanish Ministry of Science and Innovation through project ROMIAT (CTM2006-01957/MAR). This research used samples provided by the Ocean Drilling Program (ODP). The ODP is sponsored by the U.S. National Science Foundation (NSF) and participating countries under management of Joint Oceanographic Institutions (JOI). We thank J. Rolfe (U. Cambridge), T. Padró, and J. Perona (SCT-U, Barcelona) for technical assistance. We also thank R. Zahn, E. Calvo, C. Pelejero, and Eelco Rohling (Editor) for comments and scientific discussion on this manuscript.

References

Andreasen, D. J., A. C. Ravelo, and A. J. Broccoli (2001), Remote forcing at the Last Glacial Maximum in the tropical Pacific Ocean, *J. Geophys. Res.*, *106*, 879–897, doi:10.1029/1999JC000087.

Beaufort, L., T. de Garidel-Thoron, A. Mix, and N. G. Pisias (2001), ENSO-like forcing on oceanic primary production during the late Pleistocene, *Science*, *293*, 2440–2444, doi:10.1126/science.293.5539.2440.

Bostock, H. C., N. D. Opdyke, M. K. Gagan, and L. K. Fifield (2004), Carbon isotope evidence for changes in Antarctic Intermediate Water circulation and ocean ventilation in the southwest Pacific during the last deglaciation, *Paleoceanography*, *19*, PA4013, doi:10.1029/2004PA001047.

Cane, M. A. (1998), A role for the tropical Pacific, *Science*, *282*, 59–61, doi:10.1126/science.282.5386.59.

Clement, A. C., R. Seager, and M. A. Cane (1999), Orbital controls on the El Niño/Southern Oscillation and the tropical climate, *Paleoceanography*, *14*, 441–456, doi:10.1029/1999PA900013.

Clement, A. C., R. Seager, and M. A. Cane (2000), Suppression of El Niño during the mid-Holocene by changes in the Earth's orbit, *Paleoceanography*, *15*, 731–737, doi:10.1029/1999PA000466.

Chiang, J. C. H., and B. R. Lintner (2005), Mechanisms of remote tropical surface warming during El Niño, *J. Clim.*, *18*, 4130–4149, doi:10.1175/JCLI3529.1.

Conkright, M. E., R. A. Locarnini, H. E. Garcia, T. D. O'Brien, T. P. Boyer, C. Stephens, and J. I. Antonov (2002), World Ocean Atlas 2001: Objective analyses, data statistics, and figures, CD-ROM documentation, *Internal Rep. 17*, Ocean Clim. Lab., Natl. Oceanogr. Data Cent., Silver Spring, Md.

Fairbanks, R. G., M. S. Sverdlove, R. Free, P. H. Wiebe, and A. W. H. Bé (1982), Vertical distribution and isotopic fractionation of living planktonic foraminifera from the Panama Basin, *Nature*, *298*, 841–844, doi:10.1038/298841a0.

Fedorov, A. V., and S. G. Philander (2000), Is El Niño changing?, *Science*, *288*, 1997–2002, doi:10.1126/science.288.5473.1997.

Fedorov, A. V., P. S. Dekens, M. McCarthey, A. C. Ravelo, P. deMenocal, M. Barreiro, R. C. Pacanowski, and S. G. H. Philander (2006), The Pliocene paradox (mechanisms for a permanent El Niño), *Science*, *312*, 1485–1489, doi:10.1126/science.1122666.

Koutavas, A., J. Lynch-Stieglitz, T. M. Marchitto, and J. P. Sachs (2002), El Niño-like pattern in Ice Age tropical Pacific sea surface temperature, *Science*, *297*, 226–230, doi:10.1126/science.1072376.

Koutavas, A., P. deMenocal, G. C. Olive, and J. Lynch-Stieglitz (2006), Mid-Holocene El Niño–Southern Oscillation (ENSO) attenuation revealed by individual foraminifera in eastern tropical Pacific sediments, *Geology*, *34*, 993–996, doi:10.1130/G22810A.1.

Lea, D. W., D. K. Pak, and H. J. Spero (2000), Climate impact of late Quaternary equatorial Pacific sea surface temperature variations, *Science*, *289*, 1719–1724, doi:10.1126/science.289.5485.1719.

Lee, S.-Y., and C. J. Poulsen (2005), Tropical Pacific climate response to obliquity forcing in the Pleistocene, *Paleoceanography*, *20*, PA4010, doi:10.1029/2005PA001161.

Lukas, R. (1986), The termination of the equatorial undercurrent in the eastern Pacific, *Prog. Oceanogr.*, *16*, 63–90, doi:10.1016/0079-6611(86)90007-8.

Mashiotta, T., D. W. Lea, and H. J. Spero (1999), Glacial-interglacial changes in subantartic sea surface temperature and δ^{18}O-water using foraminiferal Mg, *Earth Planet. Sci. Lett.*, *170*, 417–432, doi:10.1016/S0012-821X(99)00116-8.

Ninnemann, U. S., and C. D. Charles (1997), Regional differences in Quaternary Subantartic nutrient cycling: Link to intermediate and deep water ventilation, *Paleoceanography*, *12*, 560–567, doi:10.1029/97PA01032.

Pena, L. D., E. Calvo, I. Cacho, S. Eggins, and C. Pelejero (2005), Identification and removal of Mn-Mg-rich contaminant phases on foraminiferal tests: Implications for Mg/Ca past temperature reconstructions, *Geochem. Geophys. Geosyst.*, *6*, Q09P02, doi:10.1029/2005GC000930.

Ravelo, A. C., P. S. Dekens, and M. McCarthey (2006), Evidence for El Niño–like conditions during the Pliocene, *GSA Today*, *16*, 4–11, doi:10.1130/1052-5173(2006)016<4:EFENLC>2.0.CO;2.

Rohling, E. J. (2007), Progress in paleosalinity: Overview and presentation of a new approach, *Paleoceanography*, *22*, PA3215, doi:10.1029/2007PA001437.

Shackleton, N. J., M. A. Hall, J. Line, and C. Shuxi (1983), Carbon isotope data in core V19-30 confirm reduced carbon dioxide concentration in the ice age atmosphere, *Nature*, *306*, 319–322, doi:10.1038/306319a0.

Spero, H. J., and D. W. Lea (2002), The cause of carbon isotope minimum events on glacial terminations, *Science*, *296*, 522–525, doi:10.1126/science.1069401.

Stephens, B. B., and R. F. Keeling (2000), The influence of Antarctic sea ice on glacial-interglacial CO_2 variations, *Nature*, *404*, 171–174, doi:10.1038/35004556.

Stott, L., C. Poulsen, S. Lund, and R. Thunell (2002), Super ENSO and global climate oscillations at millennial time scales, *Science*, *297*, 222–226, doi:10.1126/science.1071627.

Thunell, R. C., and L. A. Reynolds (1984), Sedimentation of planktonic foraminifera: Seasonal changes in species flux in the Panama Basin, *Micropaleontology*, *30*, 243–262, doi:10.2307/1485688.

Toggweiler, J. R. (1999), Variations of atmospheric CO_2 by ventilation of the ocean's deepest water, *Paleoceanography*, *14*, 571–588, doi:10.1029/1999PA900033.

Toggweiler, J. R., K. Dixon, and W. S. Broecker (1991), The Peru upwelling and the ventilation of the South Pacific thermocline, *J. Geophys. Res.*, *96*, 20,467–20,497, doi:10.1029/91JC02063.

Toggweiler, J. R., J. L. Russell, and S. R. Carson (2006), Midlatitude westerlies, atmospheric CO_2, and climate change during the ice ages, *Paleoceanography*, *21*, PA2005, doi:10.1029/2005PA001154.

Tsuchiya, M. (1991), Flow path of the Antarctic Intermediate Water in the western equatorial South Pacific Ocean, *Deep Sea Res., Part I*, *38*, 273–279.

Tsuchiya, M., R. Lukas, R. A. Fine, E. Firing, and E. J. Lindstrom (1989), Source waters of the Pacific Equatorial Undercurrent, *Prog. Oceanogr.*, *23*, 101–147, doi:10.1016/0079-6611(89)90012-8.

Waelbroeck, C., L. Labeyrie, E. Michel, J. C. Duplessy, J. F. McManus, K. Lambeck, E. Balbon, and M. Labracherie (2002), Sea-level and deep water temperature changes derived from benthic foraminifera isotopic records, *Quat. Sci. Rev.*, *21*, 295–305, doi:10.1016/S0277-3791(01)00101-9.

Wang, C., and P. C. Fiedler (2006), ENSO variability and the eastern tropical Pacific: A review, *Prog. Oceanogr.*, *69*, 239–266, doi:10.1016/j.pocean.2006.03.004.

Yuan, X. (2004), ENSO-related impacts on Antarctic sea ice: A synthesis of phenomenon and mechanisms, *Antarct. Sci.*, *16*, 415–425, doi:10.1017/S0954102004002238.

I. Cacho and L. D. Pena, GRC Geociències Marines, Department of Stratigraphy, Paleontology and Marine Geosciences, University of Barcelona, C/Martí i Franquès, s/n, E-08028 Barcelona, Spain. (icacho@ub.edu; lpena@ub.edu)

P. Ferretti and M. A. Hall, Godwin Laboratory for Palaeoclimate Research, Department of Earth Sciences, University of Cambridge, Downing Street, Cambridge CB2 3EQ, UK.